Available online at www.sciencedirect.com
SCIENCE DIRECT®
Biomaterials 27 (2006) 1889–1898
Biomaterials
www.elsevier.com/locate/biomaterials

Synthesis and evaluation of poly(diol citrate) biodegradable elastomers

Jian Yang, Antonio R. Webb, Samuel J. Pickerill, Gretchen Hageman, Guillermo A. Ameer*

Biomedical Engineering Department, Northwestern University, Evanston, IL 60208, USA

Received 16 March 2005; accepted 27 May 2005
Available online 15 November 2005

Abstract

Herein, we report the synthesis and evaluation of a novel family of biodegradable and elastomeric polyesters, poly(diol citrates). Poly(diol citrates) were synthesized by reacting citric acid with various diols to form a covalent cross-linked network via a polycondensation reaction without using exogenous catalysts. The tensile strength of poly(diol citrates) were as high as 11.15 ± 2.62 MPa and Young's modulus ranged from 1.60 ± 0.05 to 13.98 ± 3.05 MPa under the synthesis conditions that were investigated. Elongation was as high as $502 \pm 16\%$. No permanent deformation was found during mechanical tests. The equilibrium water-in-air contact angles of measured poly(diol citrates) films ranged from 15° to 53°. The mechanical properties, degradation and surface characteristics of poly(diol citrates) could be controlled by choosing different diols as well as by controlling the cross-link density of the polyester network. Various types of poly(diol citrate) scaffolds were fabricated to demonstrate their processing potential. These scaffolds were soft and could recover from deformation. In vitro and in vivo evaluation using cell culture and subcutaneous implantation, respectively, confirmed cell and tissue compatibility. The introduction of poly(diol citrates) will expand the repertoire of currently available biodegradable polymeric elastomers and should help meet the requirements of tissue engineering applications.

Keywords: Biodegradation; Elastomer; Scaffold; Biocompatibility; Tissue engineering

1. Introduction

The need for biodegradable polymers in emerging technologies such as tissue engineering, drug delivery, and gene therapy has been fueling a quest to develop novel biodegradable polymers [1–4]. In particular, biodegradable polymers with elastomeric properties have recently received attention for their potential use in the engineering of soft tissues such as blood vessel, heart valves, cartilage, tendon, and bladder, which exhibit elastic properties. Although a number of biodegradable elastomers have been developed [5–14], most of them require complex and costly synthesis procedures, which translate into higher manufacturing costs and hinder the commercial and clinical implementation of their use in tissue engineering.

Typically, the properties of scaffolds should resemble those of the extracelluar matrix (ECM) of the tissue or organ it is intended to replace in order to provide similar communication functions, mechanical stability and structural integrity. For example, regarding vascular tissue engineering, there is evidence that mechanical stimulation significantly regulates the phenotype of smooth muscle cells (SMC) and affects the development of smooth muscle-containing tissues [15–18]. Soft and elastomeric scaffolds are expected to be able to transfer mechanical stimuli and sustain and recovery from deformations without irritation to surrounding tissues [13]. In addition, ideal scaffold materials should be amenable to surface modification with biological adhesion and/or signaling molecules in order to overcome deleterious non-specific protein adsorption processes which may provoke undesirable cellular responses [1,19,20].

We have previously reported a novel biodegradable elastomer, poly(1,8-octanediol-*co*-citrate) (POC), which shows promise for soft tissue engineering [21,22]. Our recent efforts have focused on the investigation of a family of this type of elastomer, referred to as poly(diol citrates) in order to meet the wide-ranging needs of biomedical engineers and surgeons.

The rationale behind these elastomers is: (1) the use of non-toxic, readily available and inexpensive monomers.

*Corresponding author. Tel.: +1 847 467 6719; fax: +1 847 491 4928.
E-mail address: g-ameer@northwestern.edu (G.A. Ameer).

0142-9612/$ - see front matter © 2005 Elsevier Ltd. All rights reserved.
doi:10.1016/j.biomaterials.2005.05.106

For example, citric acid (metabolic product of the body via Kreb cycle) is chosen as a multifunctional monomer that will be reacted via polycondensation with a difunctional monomers (diol) to form a cross-linked co-polymer; (2) incorporation of homogeneous biodegradable cross-links to confer elasticity to the resulting material and leave behind some unreacted functional groups, which can be used for surface modifications; (3) the availability of various diols which provide flexibility to tune the mechanical and degradation characteristics of the resulting co-polymer, and (4) the establishment of intermolecular hydrogen bonding interactions, which should contribute to the mechanical properties of elastomers. The work herein describes the synthesis and evaluation of poly(diol citrates). The relationship between structure and function of these elastomers is also investigated.

2. Experimental

2.1. Poly(diol-citrate) synthesis

All chemicals were purchased from Sigma-Aldrich (Milwaukee, WI). Citric acid was reacted with aliphatic diols (C6–C12), N-methyldiethanolamine (MDEA), macrodiols such as poly(ethylene glycol)) and their combinations to create a polyester network with a controllable number of cross-links. Representatively, for POC synthesis [21], equimolar amounts of citric acid and 1,8-octanediol were added to a 250 ml three-neck round-bottom flask fitted with an inlet and outlet adapter. The mixture was melted at 160–165 °C under a flow of nitrogen gas while stirring. The temperature of the system was subsequently lowered to 140 °C for 30 min under stirring to create a pre-polymer. The pre-polymer was post-polymerized at either 60, 80, or 120 °C under vacuum (2 Pa) or no vacuum for times ranging from 1 day to 2 weeks to create POC with various degrees of cross-linking. For poly(1,8-octanediol-*co*-citrate-*co*-MDEA) (POCM10%) synthesis, 1,8-octanediol was partially replaced by a non-toxic monomer, MDEA [23] and then reacted with citric acid according to the above-method to obtain POCM10% (the molar ratio of MDEA:1,8-octanediol = 1:9). The following poly(diol citrates) were synthesized by post-polymerizing pre-polymers at 80 °C for 4 days: poly(1,6-hexanediol-*co*-citrate) (PHC), POC, poly(1,10-decanediol-*co*-citrate) (PDC), poly(1,12-dodecanediol-*co*-citrate) (PDDC), poly(1,8-octanediol-*co*-citrate-*co*-MDEA) (POCM10%), poly(1,12-dodecanediol-*co*-citrate-*co*-MDEA) (PDDCM10%). In addition, POC with different cross-link densities were synthesized via post-polymerization under vacuum (2 Pa) at 120 °C for 1, 3, and 6 days.

2.2. Polymer characterization

Fourier transform infrared (FTIR) spectra were obtained at room temperature using a FTS40 Fourier transform infrared spectrometer (BioRad Hercules, CA). Pre-polymer samples were prepared by a solution-casting technique (5% pre-polymer solution in 1,4-dioxane) over a KBr crystal and dried overnight under vacuum. Cross-linked poly(diol citrate) films (5 μm-thick) were cut using a microtome and placed on a KBr crystal.

^{1}H-NMR (nuclear magnetic resonance) spectra for pre-polymers were recorded on a Varian® NMR spectrometer (model Mercury 400, Palo Alto, CA) at 400 MHz. The pre-polymers were purified via precipitation in water with continuous stirring followed by freeze-drying and then dissolved in dimethyl sulfoxide-d_6 (DMSO-d_6) in 5-mm-outside-diameter tubes. The chemical shifts in parts-per-million (ppm) for ^{1}H-NMR spectra were referenced relative to tetramethylsilane (TMS, 0.00 ppm) as the internal reference.

The thermal properties of elastomers were characterized by using DSC (differential scanning calorimetry, Mettler Toledo, Columbus, OH) and TGA (thermogravimetric analysis, Mettler Toledo, Columbus, OH). For DSC measurements, samples were first scanned up to 150 °C with a heating rate of 10 °C/min under nitrogen purge (50 ml/min); thereafter cooled with a cooling rate of −40 °C/min to −60 °C and recorded a second time up to 230 °C. The glass transition temperature (T_g) was determined as the middle of the recorded step change in heat capacity from the second heating run. TGA thermograms were obtained under the flow of nitrogen gas (50 ml/min) at a scanning speed of 10 °C/min in the range of 50–600 °C. The decomposition temperature (T_d) was defined as the temperature at which 10% weight loss of the samples occurred.

Elastomer density was measured by a Mettler Toledo balance with a density determination kit (Greifensee, Switzerland) based on Archimedes' principle. Absolute ethanol was used as auxiliary liquid.

Tensile mechanical tests were conducted according to ASTM D412a on an Instron 5544 mechanical tester equipped with 500 N load cell (Instron Canton, MA). Briefly, the dog-bone-shaped sample ($26 \times 4 \times 1.5$ mm, length × width × thickness) was pulled at a rate of 500 mm/min. Values were converted to stress–strain and a Young's modulus was calculated from the initial slope. 4–6 samples were measured and averaged. The cross-link density (n) was calculated according to the theory of rubber elasticity using Eq. (1) [13,24]:

$$n = \frac{E_0}{3RT} = \frac{\rho}{M_c}, \tag{1}$$

where n represents the number of active network chain segments per unit volume (mol/m^3); M_c represents the molecular weight between cross-links (g/mol); E_0 represents Young's modulus (Pa); R is the universal gas constant (8.3144 J/mol K); T is the absolute temperature (K); and ρ is the elastomer density (g/m^3) as measured via the above method.

The water-in-air contact angles of poly(diol citrates) films were measured at room temperature using the sessile drop method [25] by a Ramé-Hart goniometer and imaging system (Ramé-Hart Inc., Mouttain Lake, NJ) within 10 s after water dropping. Four independent measurements at different sites were averaged. The contact angles changes over time were also monitored.

2.3. In vitro degradation

Disk-shaped specimens (7 mm in diameter, about 1–1.5 mm thickness) were placed in a tube containing 10 ml phosphate buffer saline (pH 7.4) or 0.1 M NaOH to rapidly obtain relative degradation rates among samples. Specimens were incubated at 37 °C in PBS or NaOH solution for predetermined times, respectively. After incubation, samples were washed with water and freeze-dried for 1 week. Mass loss was calculated by comparing the initial mass (W_0) with the mass measured at a given time point (W_t), as shown in Eq. (2). Five individual experiments were performed for the degradation test. The results are presented as means ± standard deviation.

$$\text{Mass loss}\,(\%) = \frac{W_0 - W_t}{W_0} \times 100. \tag{2}$$

2.4. In vitro cell culture

Human aortic smooth muscle cells (HASMC) and endothelial cells (HAEC) (Clonetics, Walkersville, MD) were cultured in a 50 ml culture flask with SmGM-2 and EBM-2 culture medium, respectively (Clonetics, Walkersville, MD). Cell culture was maintained in a water-jacket incubator equilibrated with 5% CO_2 at 37 °C. Cells were not used beyond passage five. Poly(diol citrate) films were cut into small pieces (1×2 cm^2) and placed in cell culture dishes (6 cm in diameter). All polymer samples were sterilized by incubation in 70% ethanol for 30 min followed by UV light exposure for another 30 min. HASMC or HAEC at a density of 1.5×10^5 cells/ml or 3×10^6 cells/ml of HAEC, respectively were added to the top of poly(diol citrate) films in tissue culture dishes (6 cm in diameter).

Approximately 30 min after cell seeding, 10 ml of culture medium were added to the culture dishes. The morphology of attached cells was observed and recorded at 24 h after cell seeding with an inverted light microscope (Nikon Eclipse, TE2000-U) equipped with a Photometrics CoolSNAP HQ (Silver Spring, MD).

2.5. Foreign body response

POC was chosen as a representative poly(diol citrate) for host response evaluation. POC disks (7 mm in diameter, 1.3 mm of thickness), sterilized via exposure to ethylene oxide gas, were implanted in 7-week-old female Sprague-Dawley rats by blunt dissection under deep isoflurane-O_2 general anesthesia. Animals were cared for in compliance with the regulations of the animal care and use committee of Northwestern University. POC disks (post-polymerized at 120°, 2 Pa, for 3 days) were implanted symmetrically on the upper and lower back of the same animal. The rats were sacrificed and tissue samples (3×3 cm) surrounding the implants were harvested with the intact implant at 1 week, 1, 2 and 4 months after implantation. The samples were fixed in 10% formalin for 24 h and embedded in paraffin after a series of dehydration steps in ethanol and xylene. The slides were stained with hematoxylin and eosin (H&E). At each time point, 3 slides (3 sections/slide) were obtained. All histologic evaluations were assessed by a trained pathologist, who was not informed of the identity of the polymer implant in each slide.

2.6. Scaffold fabrication

Porous scaffolds were fabricated based on the well-known salt-leaching method [26,27] utilizing the solubility of poly(diol citrate) pre-polymers. Pre-polymer was dissolved in 1,4-dioxane to form a 25 wt% solution, followed by addition of sieved salt which served as a porogen. The resulting slurry was cast into poly(tetrafluoroethylene) (PTFE) molds (square or tubular shapes). After solvent evaporation for 24 h, the molds were transferred into an oven for post-polymerization (80 °C, 4 days). The salt in the resulting composites was leached out by successive incubations in water (produced by Milli-Q water purification system, Billerica, MA, USA) every 12 h for 96 h. The resulting porous sponge-like films and tubular porous scaffolds were freeze-dried for 24 h and stored in a desiccator. A novel biphasic tubular scaffold for blood vessel tissue engineering was also fabricated. The biphasic scaffold consists of a non-porous skin that lines the lumen of a porous shell designed for SMC proliferation and differentiation. Briefly, for the non-porous phase, a glass rod was coated with pre-polymer and partially post-polymerized at 60 °C for 24 hr. Then, the coated rod was inserted concentrically in a tubular mold that contained a salt/pre-polymer slurry. The pre-polymer/outer-mold/glass rod system was then placed in an oven for further post-polymerization. After salt leaching, the biphasic tubular scaffold was de-molded from the glass rod and freeze-dried. All scaffold cross-sections were observed by scanning electron microscopy (SEM, Hitachi 3500 N, EPIC Northwestern University). HASMC and HAEC were seeded on biphasic scaffold and observed by SEM.

2.7. Statistical methods

Data are expressed as mean ± standard deviation. The statistical significance between two sets of data was calculated using two-tail Student's *t*-test. Data were taken to be significant, when a *P*-value of 0.05 or less was obtained.

3. Results

3.1. Polymer characterization

The purified pre-polymers were characterized by ^{1}H-NMR. Fig. 1(a) shows the ^{1}H-NMR spectra of POC. The peak at 1.53 ppm was assigned to underlined proton in –$OCH_2C\underline{H_2}$–. The multiple peaks around 2.79 ppm were assigned to the protons in –$C\underline{H_2}$– from citric acid [28]. The composition of the pre-polymer was approximately 1:1 citric acid/1,8-octanediol determined by calculating the signal intensities of both types of protons, which agreed with the initial reaction feed monomer ratio. Fig. 1(b) shows a broad peak at 3.36 ppm, which was attributed to the protons signal of –$OC\underline{H_2}CH_2$– from 1,8-octanediol and –$OC\underline{H_2}C\underline{H_2}$N- from MDEA. The peak at 3.57 ppm was partially contributed by –$C\underline{H_3}$– from MDEA [29,30].

The FTIR analysis of poly(diol citrate) elastomers are shown in Fig. 2. The peaks within 1690–1750 cm^{-1} were assigned to carbonyl (C═O) groups. A relatively broad peak centered at 1744 cm^{-1} was found in the spectra of sample A and E while in the spectra of other samples this peak was divided into fours peak, 1699, 1716, 1734, and 1749 cm^{-1} which were assigned to: (1) hydrogen bonded C═O and free C═O in ester bond and (2) hydrogen-bonded C═O and free C═O in un-reacted carboxyl group. The peaks centered at 2931 were assigned to methylene groups which were found in all the spectra of the elastomers. The broad peaks centered at 3475 and 3215 cm^{-1} were assigned to the hydrogen-bonded hydroxyl

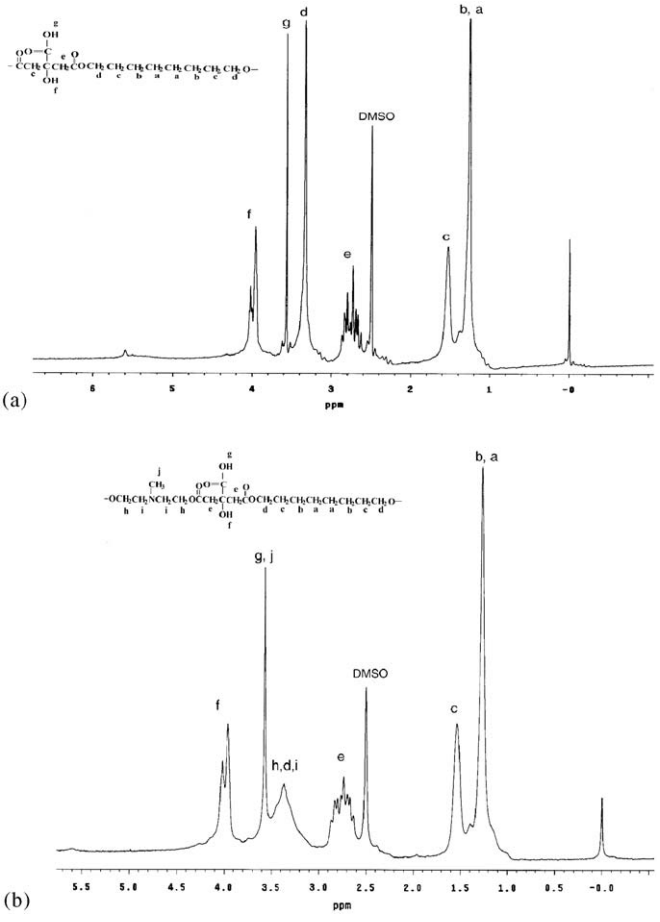

Fig. 1. ^{1}H-NMR of two representative pre-poly(diol citrates): (a) pre-POC and (b) pre-POCM10%.

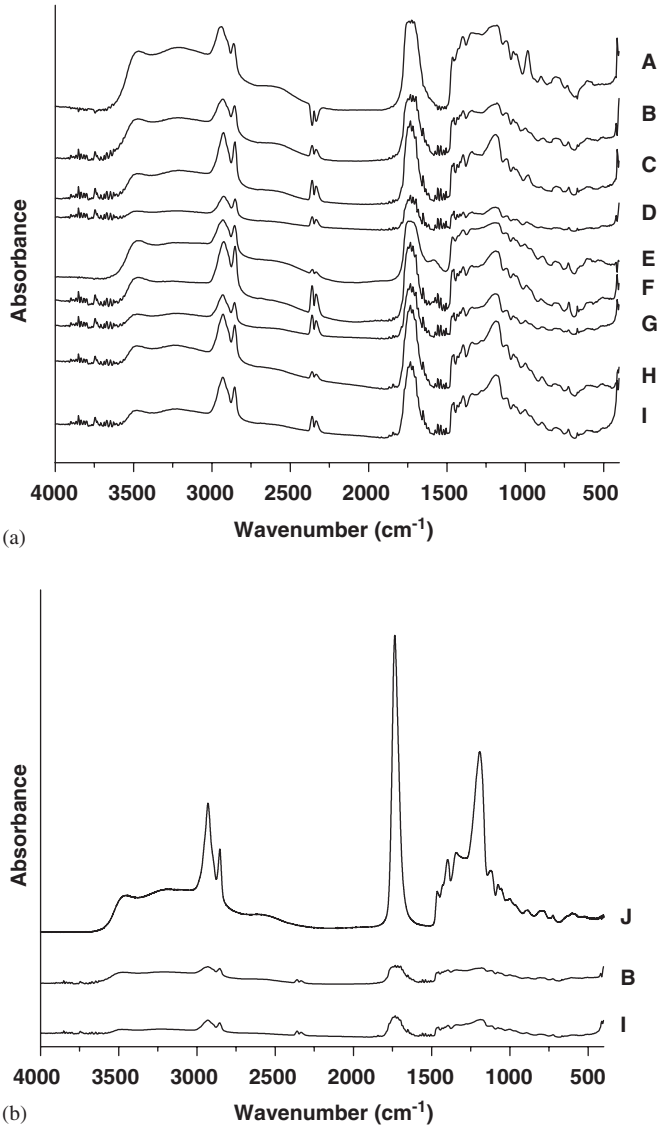

Fig. 2. (a) and (b) FTIR analysis of poly(diol citrates) which includes samples A: PHC (80 °C, 4 d); B POC (80 °C, 4 d); C PDC (80 °C, 4 d); D PDDC (80 °C, 4 d); E POCM10% (80 °C, 4 d); F PDDCM10% (80 °C, 4 d); G POC (120 °C, 2 Pa, 1 d); H POC (120 °C, 2 Pa, 3 d); I POC (120 °C, 2 Pa, 6 d); and J POC pre-polymer.

group stretching vibration and υ_{O-H} of the hydrogen-bonded carboxyl groups [31]. Fig. 2(b) shows the hydroxyl peak of sample *J*, which was much stronger than that of sample B and I. The sequences of intensity of hydroxyl peaks were pre-POC (sample J) > POC (80 °C, 4 d) (sample B) > POC (120 °C, 2 Pa, 6 d) (sample I). Initial contact angles of poly(diol citrates) increased with increasing the number of methylene units in the diol monomer. Introduction of MDEA significantly increased the initial contact angles. After 25 min, the equilibrium water-in-air contact angles of samples A, B, D, and E ranged from 15° to 53° (Table 1).

Thermal properties of poly(diol citrates) were characterized by DSC and TGA. DSC curves in Fig. 3 show apparent glass transition temperatures (T_g) for all poly (diol citrates) thermograms within −5 to 10 °C. No melting peaks or crystallization peaks were found. T_g of sample A (PHC, 9.18 °C) and sample E (POCM10%, 9.96 °C) were larger than those of the other poly(diol citrate) samples. For a same type of poly(diol citrate), increasing post-polymerization temperature and time resulted in an increase of T_g (POC samples B, G, H, and I). Thermal stability of poly(diol citrates) was characterized by TGA (Fig. 4). POCM10% and PDDCM10% were less thermally stable than other poly(diol citrates) (Fig. 4a). Increasing post-polymerization temperature and time increased the thermal stability of poly(diol citrates) (Fig. 4b).

3.2. Mechanical tests

Fig. 5 shows that tensile tests of poly(diol citrates) produced stress–strain curves characteristic of elastomeric materials. No permanent deformation was found during tensile mechanical tests (Fig. 5c). The density of poly(diol citrates) decreased gradually with increasing the number of methylene units in the diol monomer (Table 1). The tensile strength of poly(diol citrates) was as high as 11.15 ± 2.62 MPa and Young's modulus ranged from 1.60 ± 0.05 to 13.98 ± 3.05 MPa under the synthesis conditions that were investigated. Elongation was up to $502 \pm 16\%$. PHC and POCM10% had the highest tensile strength, Young's modulus and cross-link density. Increased post-polymerization temperature and time increased the tensile strength and Young's modulus while decreasing the elongation at break as reported (Fig. 5b and Table 1).

3.3. In vitro degradation studies

The data for degradation characterization of poly(diol citrates) are presented in Fig. 6. The degradation rate could be adjusted by varying the number of methylene units in the diol monomer. Diols with decreasing number of methylene units result in increasing or faster degradation rates. The introduction of MDEA into the cross-linking network significantly increased the degradation rate, while allowing the achievement of relative high tensile strength and Young's modulus.

3.4. Biocompatibility evaluation

Initial cell adhesion on poly(diol citrates) was observed 24 h after HASMC and HAEC seeding. Photomicrographs in Fig. 7 show that both types of cells attached and displayed a normal phenotype on poly(diol citrates).

The foreign body response of poly(diol citrates) was evaluated via subcutaneous implantation in Sprague-Dawley rats. POC was chosen as a representative poly(diol citrates) for evaluation. Samples that were implanted for 1 week produced a slight acute inflammatory response, which could be confirmed by the presence of leukocytes and macrophages within the tissue surrounding the co-polymer

Table 1
Density measurements, mechanical tests and cross-linking characterization of poly(diol citrates). Poly(diol citrates) were synthesized at 80 °C for 4 days except where specified otherwise

Samples	Initial contact angle (°)	Equilibrium contact angle (°)	Density (g/cm^3)	Young's modulus (MPa)	Tensile strength (MPa)	Elongation (%)	n (mol/m^3)	M_c (g/mol)
PHC	57.58±1.68	16.50±1.90	1.3022±0.0146	12.08±2.44	5.99±1.08	389±26	1650±315	789±9
POC	61.28±4.06	16.00±0.70	1.2429±0.0121	1.85±0.09	2.93±0.09	367±15	238±11	5206±51
PDC	83.10±2.03	28.7±0.80	1.1916±0.0094	1.92±0.06	3.49±0.47	338±31	247±8	4815±38
PDDC	86.43±4.27	15.23±0.55	1.1500±0.0062	1.60±0.05	6.19±1.26	502±16	206±7	5583±30
POCM10%	88.10±5.59	35.63±0.45	1.2395±0.0109	13.98±3.05	9.76±2.24	386±24	1802±393	688±6
PDDCM10%	90.10±1.02	31.5±1.5	1.1644±0.0767	4.30±0.39	11.15±2.62	445±24	555±50	2099±14
POC120, 2 Pa, 1 d	83.40±7.40	28.4±2.6	1.2260±0.0102	2.84±0.12	3.62±0.32	235±19	366±15	3348±28
POC120, 2 Pa, 3 d	89.87±2.14	27.6±0.60	1.2173±0.0049	4.69±0.48	5.34±0.66	160±15	605±62	2013±8
POC120, 2 Pa, 6 d	92.76±0.45	52.7±0.50	1.2098±0.0044	6.44±0.28	5.80±0.76	117±14	830±36	1457±5

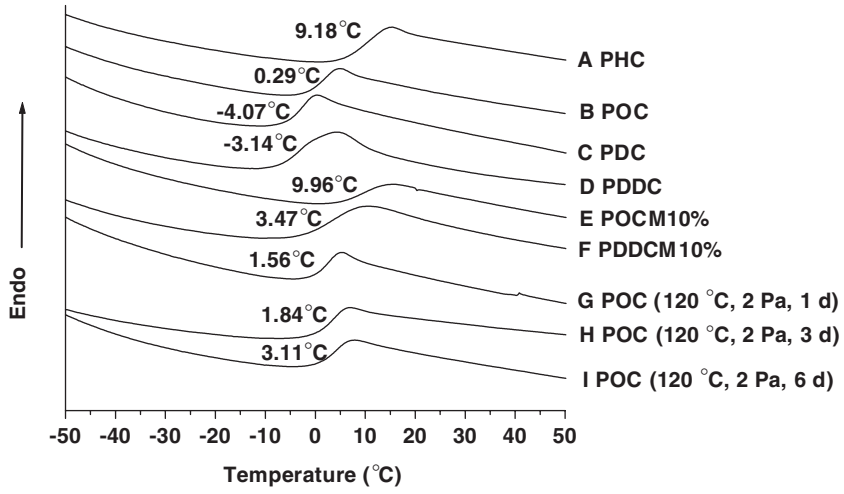

Fig. 3. DSC thermograms of poly(diol citrate). Poly(diol citrates) were synthesized at 80 °C for 4 days except where specified otherwise.

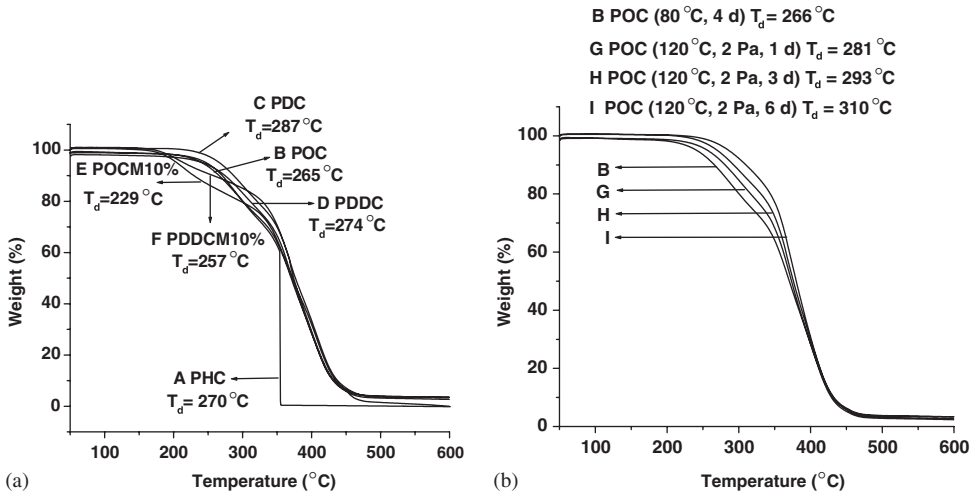

Fig. 4. TGA diagrams of poly(diol citrates). Poly(diol citrates) were synthesized at 80 °C for 4 days except where specified otherwise.

(Fig. 8a). Few macrophages were still observed surrounding the samples that were implatnted for 1 month. POC samples that were implanted for 1–4 months had a thin fibrous capsule surrounding the co-polymer. The thickness of the fibrous capsule was approximately 50 μm and did not increase significantly with time after 1 month of implantation. Blood vessels were present throughout the fibrous capsule.

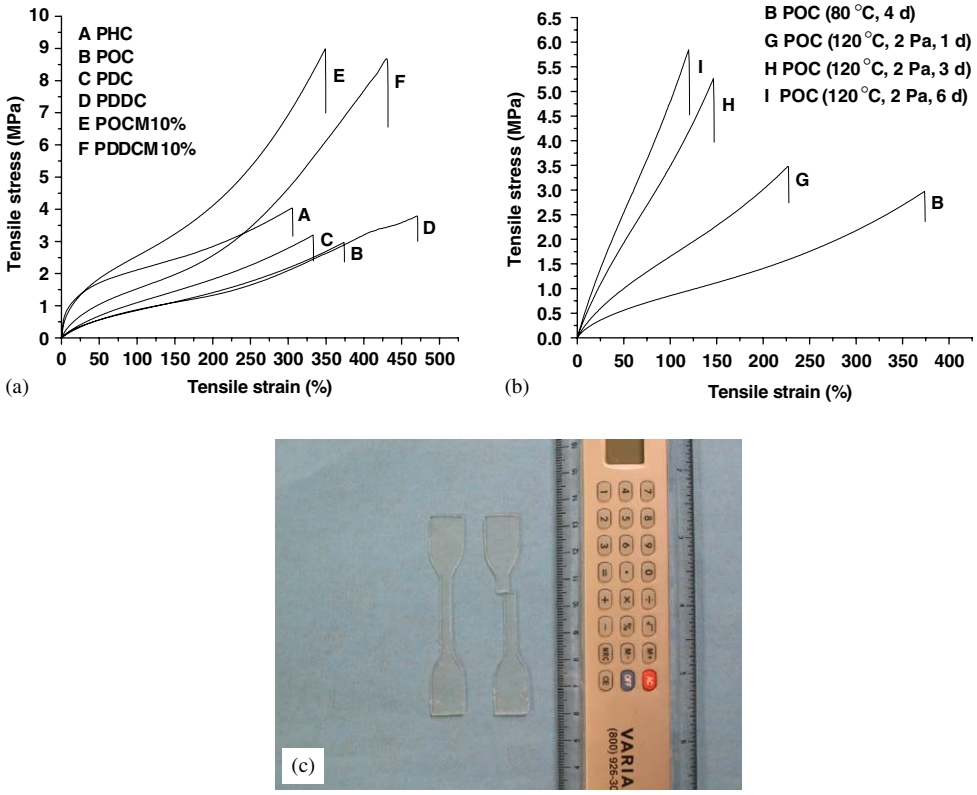

Fig. 5. (a) and (b) stress–strain curves of poly(diol citrates); (c) POC shows 100% recovery after being stretched to break. Poly(diol citrates) were synthesized at 80 °C for 4 days except where specified otherwise.

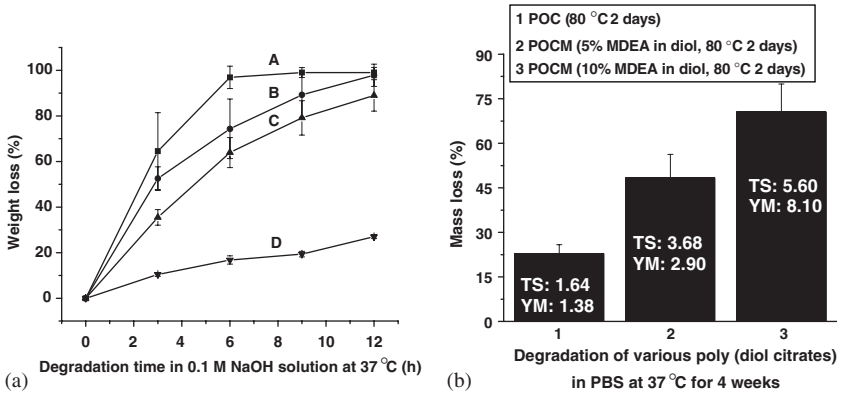

Fig. 6. Degradation studies of poly(diol citrates) in (a) 0.1 M NaOH solution and (b) PBS at 37 °C ($n = 5$). TS and YM indicate initial of tensile strength (MPa) and Young's modulus (MPa), respectively. Samples in (a) included A: PHC (80 °C, 2 d); B POC (80 °C, 2 d); C PDC (80 °C, 2 d); and D PDDC (80 °C, 2 d).

3.5. Scaffold fabrication

Poly(diol citrates) could be processed into different types of scaffolds including a novel design for vascular tissue engineering referred to as biphasic scaffold (Fig. 9a, b and e). Both, the inside non-porous phase and the outside porous phase were made of biodegradable elastomeric poly(diol citrates). Fig. 9(c, d, and f) shows the pictures of sponge-like poly(diol citrate) scaffolds with inter-connected pores. Both scaffolds types were soft and could recover from bending deformation. HASMC and HAEC cultured on a POC biphasic porous scaffold demonstrate that POC can be processed into a porous three-dimensional architecture and that cells can colonize the scaffold (Fig. 9(g, and h).

4. Discussion

Interest in engineering tissues such as blood vessel, hart valves, cartilage, and tendons has prompted the

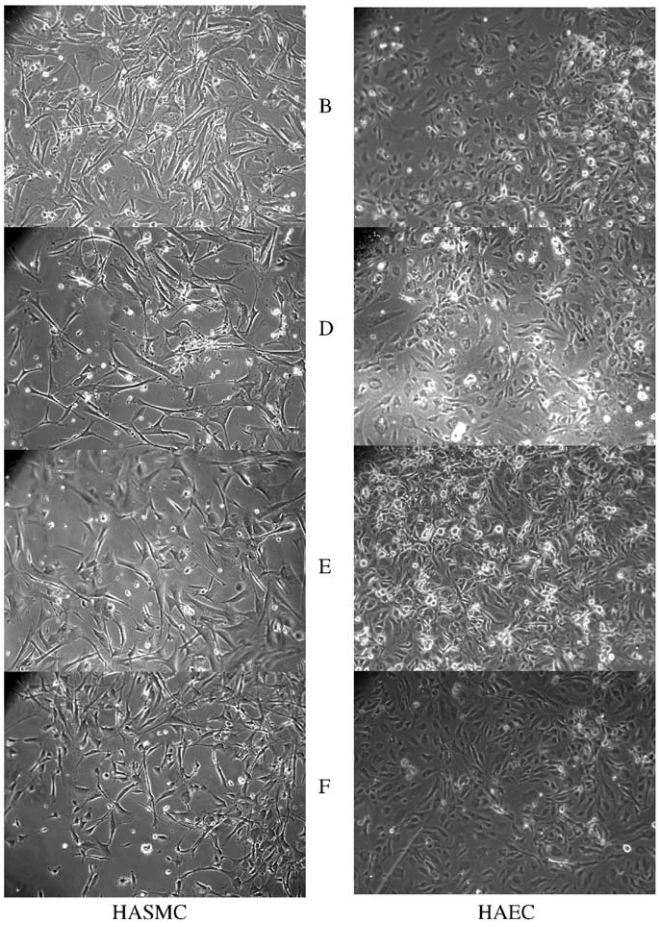

Fig. 7. Photomicrographs of HASMC and HAEC cultured on poly(diol citrates) for 24 h (× 100). Poly(diol citrates) including: B POC; D PDDC; E POCM10% and F PDDCM10% were synthesized under 80 °C, 4 d.

development of novel polyester, polycarbonate, and polyurethanes that are biodegradable and elastic. The biodegradable polyester elastomers presented in this study cover a range of mechanical properties, degradation rates, and surface energy characteristics, all of which are important to adequately control the biological response to a scaffold [1]. The relationship between structure and property was revealed through polymer characterization. Poly(diol citrates) were composed of three-dimensional polyester networks formed by reacting citric acid with various aliphatic and nitrogen-containing diols. The tertiary amine of MDEA was expected to enhance hydrogen bonding and contribute to the inclusion of positive charges in the copolymer network. Incorporation of MDEA may also modulate the charge state of the polyester network, which has been a means to regulate cell adhesion and blood vessel ingrowth within biomaterial devices [32,33].

NMR (Fig. 1) of pre-polymers that were precursors of poly(diol citrates) confirmed the selected building blocks and their ratio in the network. The changes of position and strength of FTIR peaks resulting from characteristic functional groups can be attributed to the intermolecular interactions [34]. All poly(diol citrates) showed hydrogen-bonded carbonyl groups and hydroxyl groups. For the same molar composition, PHC had a higher density of ester bonds due to the smaller number of methylene units in its monomer, 1,6-hexanediol. The introduction of MDEA in POCM10% also increased the density of ester bonds per unit volume, again likely due to the reduced number of methylene units in MDEA relative to 1,8-octanediol. FTIR spectra of PHC and POCM10% showed broadened peaks at 1744 cm^{-1} confirming the enhanced hydrogen bonding interaction. Unlike the spectra of POCM10%, the spectra of PDDCM10% still showed divided carbonyl peaks likely due to the larger number of methylene units in 1,12-dodecanediol relative to 1,8-ocatanediol in POCM10%, which partially counteracted the effects of hydrogen bonding. Increased post-polymerization temperature and reaction time resulted in an increased cross-link density and fewer un-reacted hydroxyl and carboxyl groups, as confirmed in Fig. 2(b).

The specific density of poly(diol citrates) decreased gradually with increasing number of methylene units in the diol, which was in good agreement with published results of polyester networks formed by various dicarboxylic acids and glycerol [35]. This reduction in density might be explained by an increase of the free volume of network chains between the cross-links. Mechanical properties varied depending on the selection of diols and the applied post-polymerization conditions (Fig. 5 and Table 1). The initial contact angles of poly(diol citrates) increased with the increasing number of hydrophobic methylene units. Likewise, the initial contact angles increased with increasing the reaction temperature and time, likely due to increased number of ester bonds and concomitant reduction of the un-reacted hydrophilic hydroxyl and carboxyl groups on the polymer surface. POCM10% also showed a high initial contact angle ($88.10 \pm 5.59^{\circ}$) since the introduction of MDEA also resulted in a relatively higher cross-link density. The equilibrium water-in-air contact angles after 25 min. of contact time (15°–53°) suggest that poly(diol citrates) have very good wettability even though some of them exhibited a relatively high initial contact angle, suggesting significant surface molecule re-arrangement.

The low T_g revealed by DSC analysis confirms that poly(diol citrates) are totally amorphous at 37 °C, their expected operating temperature. T_g is linked to the chain mobility of a polymer. It increases with the enhanced restriction of polymer chain mobility. The relatively higher T_g for PHC and POCM10% is attributed to the stronger intermolecular hydrogen bonding, which was confirmed by FTIR. Thus, increasing cross-link density resulted in decreased chain mobility, which in turn, increased the T_g of the polymer. The density of thermo labile ester bonds were increased by incorporating the shorter diol MDEA into the polyester network. Incorporation of this monomer lowered the thermo stability of poly(diol citrates) (Fig. 4). There were no melting peaks or crystallization peaks in all

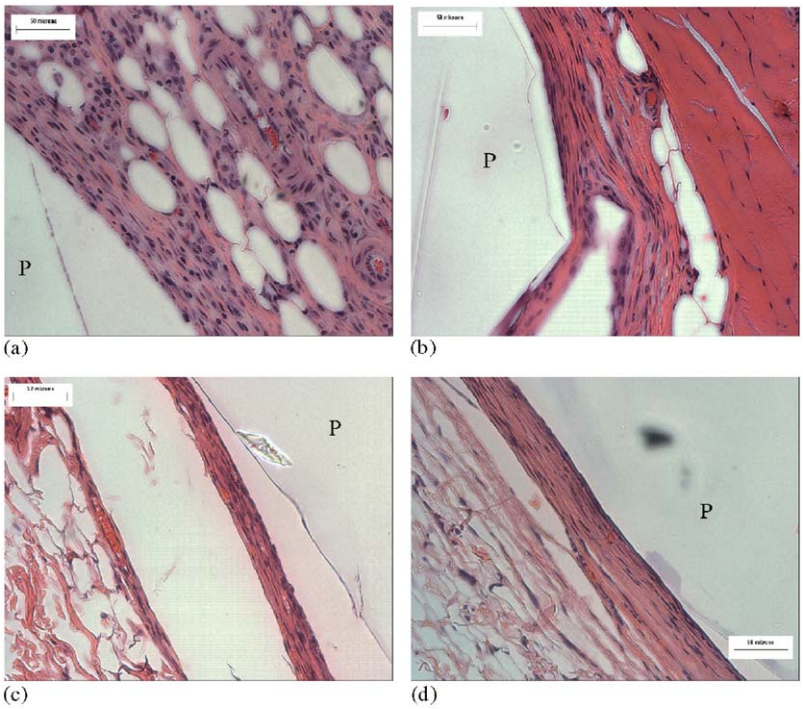

Fig. 8. Foreign body response of POC (120 °C, 2 Pa, 3 d) implanted subcutaneously in female Sprague-Dawley rats (scale bar = 50 μm). Implants and surrounding tissues were harvested after (a) 1 week; (b) 1 month; (c) 2 months; and (d) 4 months implantation for H&E staining. "P" represents polymer section.

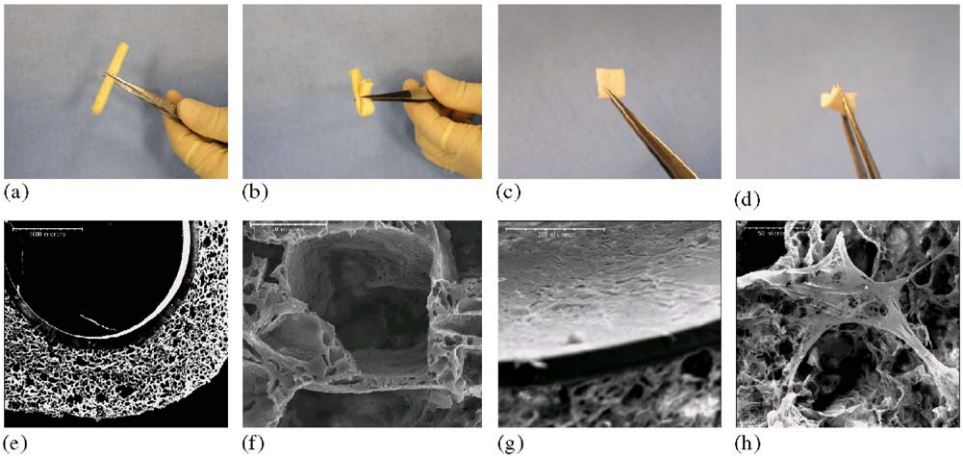

Fig. 9. (a) and (b) POC biphasic tubular scaffold; (c) and (d) POC sponge scaffold; (e) cross section of POC biphasic tubular scaffold; (f) pore structure of porous phase of biphasic scaffold (4 weeks); (g) HAEC on non-porous phase of biphasic scaffold; (h) HASMC on porous phase of biphasic scaffold (4 weeks).

DSC curves suggesting that all monomers were completely polymerized into the cross-linked network [36].

Previous results showed that a high temperature and a long post-polymerization time could result in a high tensile strength and a high Young's modulus due to high cross-link density. However, these synthesis conditions tend to produce a material that degrades very slowly [21]. Interestingly, we found that by incorporating MDEA into the co-polymer network, the mechanical properties of poly(diol citrates) could be increased, while also increasing their degradation rate (Fig. 6b). Thus, strong poly(diol citrates) with increased degradation rates can be obtained. Together with changing the selection of diol, there is significant flexibility to control the mechanical properties and degradation rates of poly(diol citrates).

Preliminary in vitro and in vivo evaluation of poly(diol citrates) confirm their potential as "cell and tissue-friendly" materials. A mild acute inflammatory response was observed at 1 week after implantation, a process that is expected and consistent with the introduction of a foreign material into the body. Macrophages were the predominant inflammatory cell type present 1 month after

implantation of the sample and by 4 months. The number of these cells was significantly reduced and localized to within the fibrous capsule surrounding the implant. Two months after the implantation, the foreign body reaction to POC produced a thin vascularized fibrous capsule that was approximately 50 μm thick. The thickness of the capsule did not change at the 4-month time point suggesting that the wound healing response had stabilized. The fibrous capsule thickness observed in this study was smaller than that reported for poly(L-lactide-*co*-glycolide) (PLGA) [37]. A thin vascularized fibrous capsule is considered to be beneficial for mass transfer between a cell-based implant and surrounding tissues. The development of a thin fibrous capsule and the time-dependent decrease of the initial mild inflammatory response suggest that POC and its degradation products are non-toxic. Therefore, poly(diol citrates) are viable candidate scaffold materials for tissue engineering, though further in vitro and in vivo evaluations would be required for the specific type of poly(diol citrate) being considered for an application. At low cross-link densities, un-reacted carboxyl and hydroxyl groups that are present on the backbone chains of the polyester network could be useful moieties for potential modification. Peptides or proteins could potentially be incorporated into the polymer surface through these groups to trigger a desired cell response [38]. Easy functionalization is an advantage of poly(diol citrates), unlike most currently used materials that need extra treatment to create chemical moieties for further biofunctionization [7,39,40].

The above characterization provides us with a comprehensive understanding of this new family of biodegradable elastomers. Poly(diol citrates) hold promise for serving as scaffold materials with tunable biodegradation and mechanical properties for soft tissue engineering. In the case of vascular tissue engineering, mechanical stimulation (such as cyclic mechanical strain) has been shown to influence the differentiation of vascular SMC and the mechanical properties of SMC-containing tissue engineered constructs [17,41,42]. Compliance mismatch between a vascular graft and a host vessel may also contribute to incomplete endothelialization and myointimal hyperplasia at the anastomotic regions [43]. Compliance of the grafts should be similar to that of the blood vessel that will be replaced, as both under compliant and overcompliant grafts may be detrimental for biomechanical adaptation [44]. This finding would imply that the compliance of a graft scaffold should be controllable to meet the needs of vascular tissue engineering [13,22]. Poly(diol citrates) were easily processed into various shapes of soft scaffolds with inter-connected pore structures, such as sponge-like scaffolds and biphasic tubular scaffolds (Fig. 9). The Young's modulus of porous poly(diol citrate) scaffolds can be adjusted to resemble that of native tissues. For example, the Young's modulus of PDDC scaffold (80 °C, 4 days) made by salt leaching combined with freeze-drying method (90% porosity, 150–250 μm pore size) is 0.50 MPa which is similar to that of human thoracic aorta (0.60 MPa) [45]. In a previous report, these scaffolds showed good fatigue resistance and the recovery from deformation was almost 100% after 500 times of compression cycles [21]. Regarding their use as cell carriers in tissue engineering, the good wettability of poly(diol citrates) is a significant advantage to achieve a uniform cell distribution during the cell seeding of a porous scaffold (data not shown). In this study, vascular cells were seeded on biphasic tubular scaffolds, which consisted of a non-porous and porous phases to enable cell compartmentalization. The non-porous phase of a biphasic tubular scaffold is expected to provide a continuous surface for EC adhesion and spreading, mechanical strength, and elasticity to the scaffold. The porous phase is expected to facilitate the 3-D proliferation of SMC. The detailed design and evaluation of a biphasic scaffold for small-diameter blood vessel tissue engineering is published elsewhere [46].

Lastly, poly(diol citrates) could not only be used in their pure form in a final product or device, but also have great potential to form composite materials with improved mechanical and cell compatible properties depending on the application. We have prepared poly(diol citrates)-HA (hydroxyapatite), poly(diol citrates)-chitosan, and poly(-diol citrates)-PLA (polylactide) composites with properties that are relevant to orthopedic and vascular tissue engineering applications (data not shown here). These composites have different physical and chemical properties from their components; in particular strength and elasticity were conferred. Composite materials of poly(diol citrates) are under active investigation in our lab for various biomedical applications.

5. Conclusions

Poly(diol citrates) elastomers exhibit controllable biodegradation and mechanical properties via a simple, safe and cost-effective polycondensation reaction. Poly(diol citrates) were confirmed to be compatible with vascular cells and subcutaneous tissue and were processed into various types of scaffold for soft tissue engineering. The introduction of poly(diol citrates) should expand the repertoire of available biodegradable polymeric elastomers to meet the requirements of tissue engineering and other biomedical applications.

Acknowledgements

This work was funded in part through a grant by American Heart Association and The National Institutes of Health (R21-HL071921-02).

References

[1] Ratner BD, Bryant SJ. Biomaterials: where we have been and where we are going. Annu Rev Biomed Eng 2004;6:41–75.
[2] Lavik E, Langer R. Tissue engineering: current state and perspectives. Appl Microbiol Biotechnol 2004;65:1–8.

[3] Okada M. Chemical syntheses of biodegradable polymers. Prog Polym Sci 2002;27:87–133.
[4] Griffith LG. Polymeric biomaterials. Acta Mater 2000;48:263–77.
[5] Jeong SI, Kim SH, Kim YH, Jung YM, Kwon JH, Kim BS. Manufacture of elastic biodegradable PLCL scaffolds for mechano-active vascular tissue engineering. J Biomater Sci Polymer Edn 2004; 15:645–60.
[6] Younes H, Bravo-Grimaldo E, Amsden B. Synthesis, characterization and in vitro degradation of a biodegradable elastomer. Biomaterials 2004;25:5261–9.
[7] Guan J, Sacks MS, Beckman EJ, Wagner WR. Biodegradable poly(ether ester urethane)urea elastomers based on poly(ether ester) triblock copolymers and putrescine: synthesis, characterization and cytocompatibility. Biomaterials 2004;25:85–96.
[8] Sung HJ, Meredith C, Johnson C, Galis ZS. The effects of scaffold degradation rate on three-demensional cell growth and angiogenesis. Biomaterials 2004;25:5735–42.
[9] Pêgo AP, Poot AA, Grijpma DW, Feijen J. Biodegradable elastomeric scaffolds for soft tissue engineering. J Control Release 2003;87:69–79.
[10] Kweon H, Yoo MK, Park IK, Kim TH, Lee HC, Lee HS, et al. A novel degradable polycaprolactone networks for tissue engineering. Biomaterials 2003;24:801–8.
[11] Saad B, Neuenschwander P, Uhlschmid GK, Suter UW. New versatile, elastomeric, degradable polymeric materials for medicine. Int J Biol Macromol 1999;25:293–301.
[12] Skarja GA, Woodhouse KA. Structure-property relationships of degradable polyurethane elastomer containing an amino acid-based chain extender. J Appl Polym Sci 2000;75:1522–34.
[13] Wang Y, Ameer GA, Sheppard B, Langer R. A tough biodegradable elastomer. Nat Biotechnol 2002;20:587–91.
[14] Yang J, Webb AR, Ameer GA. Biodegradable elastomeric polymers for tissue engineering. In: Mallapragada SK, Narasimhan B, editors. Handbook of biodegradable polymeric materials and their applications. USA: American Scientific Publishers; 2005. p. 191–232.
[15] Kim BS, Nikolovski J, Bonadio J, Mooney DJ. Cyclic mechanical strain regulates the development of engineered smooth muscle tissue. Nat Biotechnol 1999;17:979–83.
[16] Kim BS, Mooney DJ. Scaffolds for engineering smooth muscle under cyclic mechanical strain conditions. J Biomech Eng 2000;122: 210–5.
[17] Stegemann JP, Nerem RM. Phenotype modulation in vascular tissue engineering using biochemical and mechanical stimulation. Ann Biomed Eng 2003;31:391–402.
[18] Solan A, Mitchell S, Moses M, Niklason L. Effect of pulse rate on collagen deposition in the tissue-engineered blood vessel. Tissue Eng 2003;9:579–86.
[19] Shin H, Jo S, Mikos AG. Biomimetic materials for tissue engineering. Biomaterials 2003;24:4353–64.
[20] Hersel U, Dahmen C, Kessler H. RGD modified polymers: biomaterials for stimulated cell adhesion and beyond. Biomaterials 2003;24:4385–415.
[21] Yang J, Webb AR, Ameer GA. Novel citric acid-based biodegradable elastomers for tissue engineering. Adv Mater 2004;16:511–6.
[22] Webb AR, Yang J, Ameer GA. Biodegradable polyester elastomers in tissue engineering. Expert Opin Biol Ther 2004;4:801–12.
[23] Wang C, Ge Q, Ting D, Nguyen D, Shen H, Chen J, et al. Molecularly engineered poly(ortho ester) microspheres for enhanced delivery of DNA vaccines. Nat Mater 2004;3:190–6.
[24] Sperling LH. Introduction to physical polymer science. New York: Wiley; 1992.
[25] Yang J, Bei J, Wang S. Enhanced cell affinity of poly (D,L-lactide) by combining plasma treatment with collagen anchorage. Biomaterials 2002;23:2607–14.
[26] Yang J, Shi G, Bei J, Wang S, Cao Y, Shang Q, et al. Fabrication and surface modification of macroporous poly(L-lactic acid) and poly(L-lactic-*co*-glycolic acid) (70/30) cell scaffolds for human skin fibroblast cell culture. J Biomed Mater Res 2002;62:438–46.
[27] Widmer MS, Gupta PK, Lu LC, Meszlenyi RK, Evans GRD, Brandt K, et al. Manufacture of porous biodegradable polymer conduits by an extrusion process for guided tissue engineering. Biomaterials 1998;19:1945–55.
[28] Barroso-Bujans F, Martinez R, Ortiz P. Stuctural characterization of oligomers from the polycondensation of citric acid with ethylene glycol and long-chain aliphatic alcohols. J Appl Polym Sci 2003;88:302–6.
[29] Bishnoi S, Rochelle GT. Thermodynamics of piperazine/methyldiethanolamine/water/carbon dioxide. Ind Eng Chem Res 2002;41: 604–12.
[30] Al-Salah HA. Synthesis and properties of liquid-crystalline polyetherurethane cationomers. Acta Polym 1998;49:465–70.
[31] Xie D, Chen D, Jiang B, Yang C. Synthesis of novel compatibilizers and their application in PP/nylon-66 blends. I. Synthesis and characterization. Polymer 2000;41:3599–607.
[32] Yang J, Bei J, Wang S. Improving cell affinity of poly(D,L-lactide) film modified by anhydrous ammonia plasma treatment. Polym Adv Technol 2002;13:220–6.
[33] Sanders JE, Lamont SE, Karchin A, Golledge SL, Ratner BD. Fibroporous meshes made from polyurethane micro-fibers: effects of surface charge on tissue response. Biomaterials 2005;26:813–8.
[34] Li J, He Y, Inoue Y. Thermal and infrared spectroscopic studies on hydrogen-bonding interactions between poly (caprolactone) and some dihydric phenols. J Polym Sci Part B: Polym Phys 2001;39: 2108–17.
[35] Nagata M, Kiyotsukuri T, Ibuki H, Tsutsumi N, Sakai W. Synthesis and enzymatic degradation of regular network aliphatic polyesters. React Funct Polym 1996;30:165–71.
[36] Ju YM, Ahn KD, Kim JM, Hubbell JA, Han DK. Physical properties and biodegradation of lactide-based poly(ethylene glycol) polymer networks for tissue engineering. Polym Bull 2003;50:107–14.
[37] Cadee JA, Brouwer LA, Otter WD, Hennink WE, van Luyn MJA. A comparative biocompatibility study of microsphere based on cross-linked dextran or poly(lactic-*co*-glycolic)acid after subcutaneous injection in rats. J Biomed Mater Res 2001;56:600–9.
[38] Hirano Y, Mooney DJ. Peptide and protein presenting materials for tissue engineering. Adv Mater 2004;16.
[39] Yang J, Wan YQ, Yang JL, Bei JZ, Wang SG. Plasma treated, collagen anchored polylactone: its cell affinity evaluation under shear or shear free conditions. J Biomed Mater Res 2003;67A:1139–47.
[40] Zhu Y, Gao C, He T, Shen J. Endothelium regeneration on luminal surface of polyurethane vascular scaffold modified with diamine and covalently grafted with gelatin. Biomaterials 2004;25:423–30.
[41] Lee SH, Kim BS, Kim SH, Choi SW, Jeong SI, Kwon IK, et al. Elastic biodegradable poly(glycolid-*co*-caprolactone) scaffold for tissue engineering. J Biomed Mater Res 2003;66A:29–37.
[42] Nerem RM. Role of mechanics in vascular tissue engineering. Biorheology 2003;40:281–7.
[43] Xue L, Greisler HP. Biomaterials in the development and future of vascular grafts. J Vasc Surg 2003;37:472–80.
[44] He H, Matsuda T. Arterial replacement with compliant hierarchic hybrid vascular graft: biomechancial adaptation and failure. Tissue Eng 2002;8:213–24.
[45] O'Rourke MF, Staessen JA, Vlachopoulos C, Duprez D, Plante GE. Clinical applications of arterial stiffness; definitions and reference values. Am J Hypertens 2002;15:426–44.
[46] Yang J, Motlagh D, Webb AR, Ameer GA. A novel biphasic elastomeric scaffold for small-diameter blood vessel tissue engineering. Tissue Eng 2005, in press.